

Quantum Light on Demand

Mithilesh K. Parit,^{1,*} Shaik Ahmed,² Sourabh Singh,¹ P. Anantha Lakshmi,^{3,†} and Prasanta K. Panigrahi^{1,‡}

¹*Department of Physical Sciences, Indian Institute of Science Education
and Research Kolkata, Mohanpur-741246, West Bengal, India*

²*Department of Humanities and Science, MLR Institute of Technology, Dundigal, Hyderabad-500043, Telangana, India*

³*School of Physics, University of Hyderabad, Hyderabad - 500046, Telangana, India*

(Dated: January 27, 2023)

The far field radiation pattern of three dipole coupled, two level atoms is shown to yield sub and super radiant behavior, with the nature of light quanta controlled by the underlying quantum correlations. Superradiance is found to faithfully reflect the monogamy of quantum correlation. It persists at higher temperatures with reduced intensity, even in the absence of entanglement but with non-zero quantum discord. This establishes the physical manifestation of quantum discord. The intensity of emitted radiation is highly focused and anisotropic in one phase and completely uniform in another, with the two phases separated by a crossover. Radiated intensity is shown to exhibit periodic variation from super to sub-radiant, as a function of inter atomic spacing and observation angle, which persists up to significantly high temperatures. The precise effects of transition frequency and inter-dipole spacing on the angular spread and variations of the intensity in the uniform and non-uniform regimes are explicitly demonstrated at finite temperature. Photon-photon correlation is shown to exhibit sub- and super Poissonian statistics in a parametrically controlled manner.

keywords: Two-level atoms, Superradiance, Quantum discord, Entanglement

PACS numbers: 03.65.Ud , 03.67.-a, 42.50.Ar

I. INTRODUCTION

Light of desired nature is much in demand for both fundamental [1, 2] and technological applications [3]. Study of coherent and incoherent sources of light, as well as sources generating single [4, 5] and entangled photons are subjects of intense investigation [6–15]. The detection, characterization [12, 13], and control of light have attracted significant attention. In this regard, light emission from entangled sources is being studied with particular interest, for its superradiant character, originally predicted by Dicke in 1954 [16]. Apart from dramatic enhancement of intensity, the emitted radiation provides much room for controlling its property.

Dicke superradiance is the coherent spontaneous emission from a many-body system, owing its origin to the co-operative simultaneous interaction among its constituents, all of them experiencing a common radiation field [16]. The collective behavior of the ensemble arises from the coherent superposition and entanglement structure of the many-body wave function. The correlated structure can also show subradiant behavior due to destructive interference of the superposition states. It is interesting to note that some of the excited and ground states in the original study of Dicke are highly entangled [17]. Superradiance has been extensively studied in the literature, with the identification of

a phase transition, separating the coherent phase of radiation from its incoherent counterpart [18–20]. It has attracted significant interest due to its possible applications, ranging from generation of X-ray lasers with high powers [21], short pulse generation [22] to self-phasing in a system of classical oscillators [23], to name a few. Super- and sub-radiant behavior has been investigated experimentally in many physical systems [24–29]. In particular, Dimitrova et al. [27] observed superradiance in a Bose-Einstein condensate (BEC). In yet another study, superfluidity of BEC along the axis of ring cavity has been shown to yield superradiant scattered photons [29].

In the context of quantum information, it is of particular interest to explore how the behavior of radiation field gets affected for a collection of atoms, when the quantum states are correlated in different ways. This allows for optical probing of quantum correlations (QCs) and aids in quantifying QCs that may be present in the system. It is well understood that depending on the nature of interactions of the multi-particle system, one can realize different types of entangled states [30, 31] leading to different radiation characteristics. These atomic entangled states can find potential applications in quantum information processing [32], for generating different entangled quantum states of light for quantum memories [33, 34], quantum communication [35], and quantum cryptography [36, 37], among others.

Two particle entanglement has been well characterized both for pure and mixed states [38], using different measures viz., von Neumann entropy and concurrence. Recently, concurrence [39, 40] and quantum discord

* mithilesh.parit@gmail.com, mkp13ms113@iiserkol.ac.in

† pochincherla03@gmail.com, palasp@uohyd.ernet.in

‡ pprasanta@iiserkol.ac.in, panigrahi.iiser@gmail.com

[41] have been used for quantitatively characterizing entanglement governing the quantum phase transition occurring in an antiferromagnetic spin chain, consisting of weakly coupled dimers [38–41]. In comparison, the three particle entanglement is much less understood. It is known to exhibit stronger QCs as compared to the Bell states and also shows stronger non-locality [42]. The entanglement structure of multiparticle states of different type are yet to be completely understood [43]. Here, we investigate the effect of entanglement, quantum discord, and monogamy relations on sub- and super-radiance of three two-level atom system.

Recently, Wiegner et al. [17] have investigated the super and sub-radiant characteristics of an N -atom system in a generalized W -state of the form $\frac{1}{\sqrt{n}}|j, n-j\rangle$, with j atoms in the excited state and $(n-j)$ atoms in the ground state, where the role of entanglement has been highlighted for pure states. In another study, the effect of quantum discord on super- and sub-radiant intensities in a system of X -type quantum states has been investigated [44], without taking into account the effect of finite temperatures. In the present study, we carry out a systematic investigation of the sub- and super-radiant properties of three correlated two level atoms and explore the effect of inter atomic spacing, on the resulting radiation pattern. More specifically, the precise role of transition frequency and inter-dipole spacing on the nature of intensity, photon-statistics, and angular spread of emitted radiation are explicitly demonstrated. The behavior of radiation field pattern as a function of concurrence and quantum discord is probed for gaining a physical understanding of the effect of different QCs on the emitted light. The role of QCs in producing highly collimated light, as well as completely uniform illumination is illustrated. The connection of entanglement on far field radiation pattern is demonstrated for two different configurations, originating from the two topologically different arrangements of atoms differing in their coupling pattern and phase structure. The photon-photon correlation, as a function of system parameters, is found to yield sub- and super- Poissonian characteristics.

The paper is organized as follows. In Sec. II, the Hamiltonian for the system of three identical two-level atoms interacting via dipole-dipole coupling is introduced, using pseudo spin variables. We present exact results at non-zero temperature for the intensity of the emitted radiation from the three two-level atoms arranged in line configuration in Sec. III. This is followed in Sec. IV by the investigation of radiation intensity from the loop configuration, where atoms are placed on vertices of an equilateral triangle. Finally, we conclude with a summary of the results and direction for future research.

II. THEORY AND MODEL

We consider a system of three coupled identical atoms, where the excited state $|e_i\rangle$ and the ground state $|g_i\rangle$, $i = 1, 2, 3$ are separated by an energy interval $\hbar\omega$ ($\hbar = 1$ in our case). The Hamiltonian for the system of three identical two-level atoms coupled through dipole-dipole interaction is given by,

$$H = \sum_{i=1}^3 \omega_i S_i^z + \sum_{i \neq j=1}^3 \Omega_{ij} S_i^+ S_j^-. \quad (1)$$

The first term describes the unperturbed energy of the system and the second term represents the dipole-dipole interaction between the ground state of one atom and the excited state of another atom, where, Ω_{ij} , the dipole-dipole interaction strength, which is a function of the inter-atomic separation ' d '. The nature of dipole-dipole interaction prohibits interaction between two atoms which are both in excited/ground state. In the above, $S_i^+ = |1\rangle_i \langle 0|$ and $S_i^- = |0\rangle_i \langle 1|$ are the raising and lowering operators of the i^{th} atom in the spin representation. Our system is closed and non-interactive with environment, which can be extended to open system dynamics [45, 46].

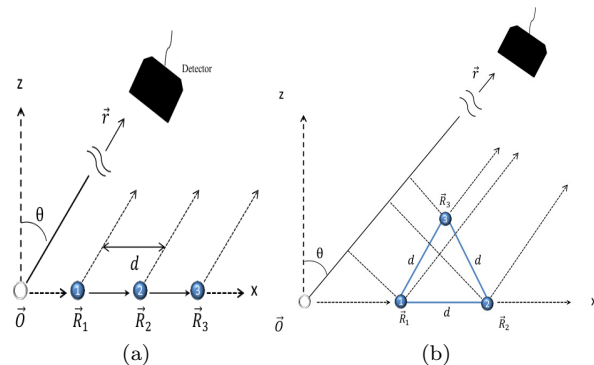


FIG. 1. (Color online) Schematic diagram of the system in the line and loop configurations with identical two-level atoms localized at positions (a) \vec{R}_1 to \vec{R}_3 and (b) atoms at the vertices of an equilateral triangle with a detector at position \vec{r} .

Two possible inequivalent configurations namely, open loop (line) and closed loop (loop) exist, for which the nature of entangled states are different. The nature of coupling between the atoms of these two distinct configurations is different, giving rise to distinct differences in the resulting field intensities. The presence of the coupling, Ω_{ij} , between the atoms causes mixing of the energy levels, leading to the creation of states with different correlations.

We investigate the intensity emitted by three atom system, in the far field zone i. e., $\vec{r} \gg d$; where d is spacing

between the atoms and \vec{r} denotes the position of the detector to record the photons emitted by the atoms in the far field regime. The positive frequency component of the electric field operator [2, 17] is given by

$$\hat{E}^{(+)} = -\frac{e^{ikr}}{r} \sum_j \vec{n} \times (\vec{n} \times \vec{p}_{ge}) e^{-i\phi_j} \hat{S}_j^-, \quad (2)$$

where \vec{r} indicates the detector position, the unit vector $\vec{n} = \frac{\vec{r}}{r}$ and \vec{p}_{ge} , the dipole moment of the atomic transition $|e\rangle \rightarrow |g\rangle$. Here ϕ_j is the relative optical phase accumulated by a photon emitted at \vec{R}_j and detected at \vec{r} .

We also assume \vec{p}_{ge} to be oriented along the y-direction and \vec{n} in the x-z plane, resulting in vanishing $\vec{p}_{ge} \cdot \vec{n}$. These assumptions, together with the normalization, give rise to dimensionless expressions for the amplitude as,

$$\hat{E}^{(+)} = \sum_j e^{-i\phi_j} \hat{S}_j^-, \quad (3)$$

resulting in the following expression for the radiated intensity at \vec{r} :

$$\begin{aligned} I(\vec{r}) &= \langle \hat{E}^{(-)} \hat{E}^{(+)} \rangle = \sum_{i,j} \langle \hat{S}_i^+ \hat{S}_j^- \rangle e^{i(\phi_i - \phi_j)} \\ &= \sum_i \langle \hat{S}_i^+ \hat{S}_i^- \rangle + \left(\sum_{i \neq j} \langle \hat{S}_i^+ \rangle \langle \hat{S}_j^- \rangle + \right. \\ &\quad \left. \sum_{i \neq j} (\langle \hat{S}_i^+ \hat{S}_j^- \rangle - \langle \hat{S}_i^+ \rangle \langle \hat{S}_j^- \rangle) e^{i(\phi_i - \phi_j)} \right). \end{aligned} \quad (4)$$

Thus, the characteristics of the intensity would depend on the incoherent terms $\langle \hat{S}_i^+ \hat{S}_i^- \rangle$, the non vanishing of the dipole moments $\langle \hat{S}_i^+ \rangle$, and the QCs of the form $\langle \hat{S}_i^+ \hat{S}_j^- \rangle - \langle \hat{S}_i^+ \rangle \langle \hat{S}_j^- \rangle$.

We now take into account the thermal effects, where, at finite temperature, the expectation value of an observable $\langle \hat{A} \rangle$ takes the form

$$\langle \hat{A} \rangle = \text{Tr}(\hat{\rho} \hat{A}), \quad (5)$$

with $\hat{\rho}$ being the thermal density operator given by

$$\hat{\rho} = \frac{\sum_{i=1}^8 |\psi_i\rangle \langle \psi_i| e^{-\beta \epsilon_i}}{\text{Tr} \left(\sum_{i=1}^8 |\psi_i\rangle \langle \psi_i| e^{-\beta \epsilon_i} \right)}. \quad (6)$$

Here $|\psi_i\rangle$ is an eigenstate with ϵ_i its eigenvalue. Additional information on $|\psi_i\rangle$ and ϵ_i along with $\hat{\rho}$ for

both the configurations is provided in supplementary material. In the ensuing sections, we investigate the intensity pattern resulting from the loop and line configurations as a function of the system parameters, as well as the inter atomic distance and observation angle.

III. THE INTENSITY CHARACTERISTICS OF THE LINE-CONFIGURATION

In the line configuration, a system of three identical dipole coupled two-level atoms are placed symmetrically along a line. For simplicity, we consider the transition frequencies of all the three atoms to be the same, $\omega_1 = \omega_2 = \omega_3 = \omega$ and the nearest neighbor dipole-dipole interactions $\Omega_{12} = \Omega_{23} = \Omega = 1$ and $\Omega_{13} = 0$. As depicted in Fig. 8(a), atoms are localized at positions R_1, R_2 and R_3 , with equal spacing d between adjacent atoms.

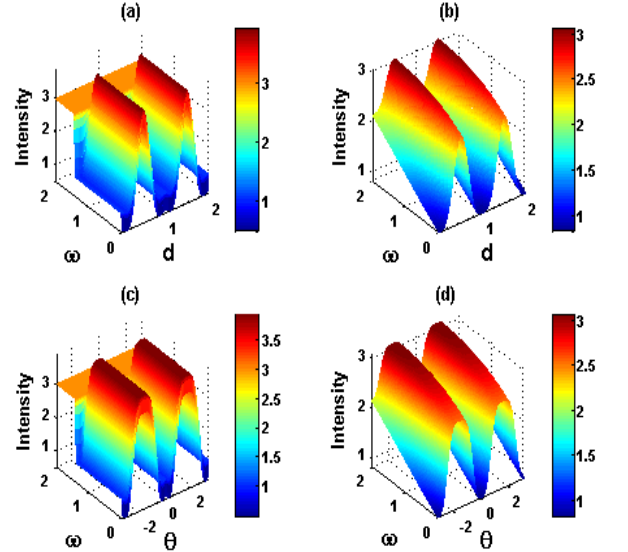


FIG. 2. (Color online) Panels *a* and *b* show the intensity variation at fixed temperature and observation angle ($\theta = \frac{\pi}{2}$) as a function of inter-atomic spacing and transition frequency for (a) $T=0.005$ and (b) $T=1$. Panels *c* and *d* show the radiation intensity for fixed inter-atomic spacing ($d = \frac{\lambda}{2}$) as a function of observation angle and transition frequency for (c) $T=0.005$ and (d) $T=1$, clearly revealing two distinct phases and interference effect.

For this topology, ϕ_j , the relative optical phase accumulated by a photon emitted at \vec{R}_j and detected at \vec{r} is

$$\phi_j(\vec{r}) \equiv \phi_j = k\vec{n} \cdot \vec{R}_j = jkd \sin \theta. \quad (7)$$

The exact expression for the intensity for three atoms arranged along a line is derived by combining Eqs. (4)

to (7) and is given in the supplementary information.

In an earlier work, the role of entanglement on super- and sub-radiant behavior for the three atom system, with a zero net dipole moment, was studied [17]. Here, we have generalized this study, exhibiting the presence of QCs and their physical effect for the three atom system. Fig. 2 depicts the periodic variation in the intensity from super to subradiant behavior as a function of transition frequency and inter-atomic spacing/observation angle. This reflects the subtle interference effects present in the three particle system. For high ω and at low temperatures, a phase with uniform light emission is seen, separated from a non-uniform intensity with periodic modulations. The uniform phase (emission) of radiation arises when both entanglement and discord vanish, as is evident from Figs. 2(a), 2(c), and 3(c). A smooth crossover connects the two phases. The plot of crossover of eigen-energies is presented in the supplementary material. The uniform phases vanish at higher temperatures as can be seen in Figs. 2(b) and 2(d).

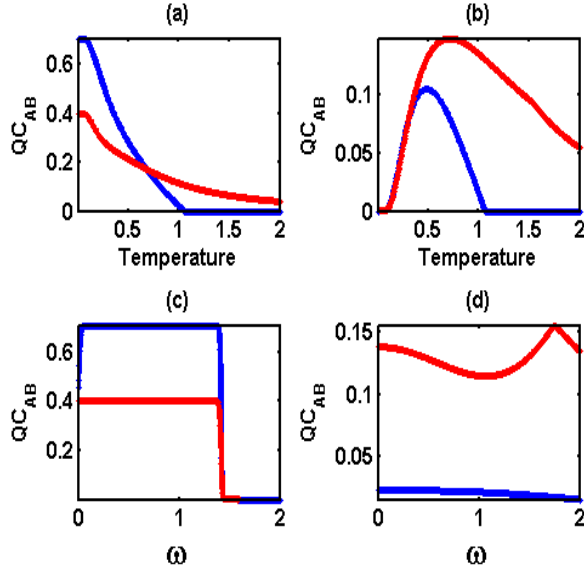


FIG. 3. (Color online) Panels *a* and *b* show the variation of QCs (Concurrence (blue) and Discord (red)) as a function of temperature for different transition frequencies (a) $\omega = 1$ and (b) $\omega = 2$. Panels *c* and *d* show the variation of QCs as function of transition frequency for different temperatures (c) $T = 0.005$ and (d) $T = 1$, showing vanishing of QCs at high ω and low temperatures.

To understand the intensity profile, for the given system, it is imperative to know the variation of QCs with temperature and transition frequency. In Fig. 3, panels *a* and *b* show the behavior of concurrence [47] and quantum discord [48–50] as a function of temperature, for two different values of the transition frequencies,

while panels *c* and *d* show the variation of QCs as function of transition frequency for different temperatures. For small value of transition frequency (temperature), increasing the temperature (transition frequency) leads to reduction in the value of both concurrence and discord, with concurrence vanishing for $T = 1$ but discord remaining non-zero beyond this temperature. Thus, the intensity pattern at small T and small values of ω observed in Fig. 2 is predominantly due to the high amount of QCs present in the system. This result also confirms that even for $T > 1$, the superradiant behavior is present, albeit with reduced intensity in the absence of concurrence but with non-zero discord as is evident from Figs. 2 and 3. This explicates the physical significance of quantum discord. The blue region in the plot represents subradiant behavior, while the red regions correspond to superradiant behavior. Fig. 2 clearly shows that the spacing between atoms and observation angle play significant role for emission and detection of superradiant light. The intensity is maximum at inter-dipole spacing $d = (2n+1)\frac{\lambda}{2}$, at the specific value of the observation angle $\theta = \frac{\pi}{2}$. The intensity pattern for different combinations of θ and d is shown in Fig. 4 (including $\theta = \pm\frac{\pi}{2}$ and $d = (2n+1)\frac{\lambda}{2}$ with $n = 0, 1, 2, \dots$).

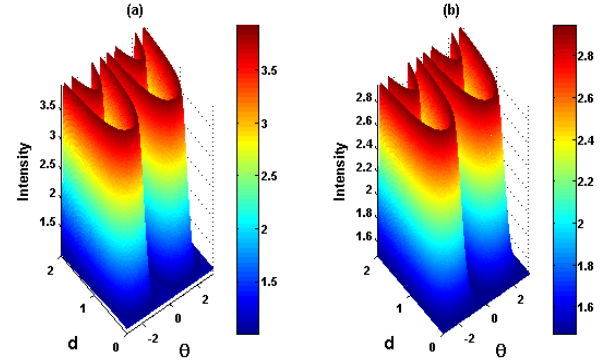


FIG. 4. (Color online) The periodic variation of intensity is shown as a function of observation angle and spacing between atoms at fixed transition frequency ($\omega = 1$) for different temperatures of magnitude (a) $T = 0.005$ and (b) $T = 1$.

The behavior of intensity as a function of observation angle and inter-atomic spacing at fixed transition frequency ($\omega = 1$), for different temperatures is shown in Fig. 4. Sub- and super-radiant nature of radiation is observed for all inter-atomic distances and observation angles (except for $\theta = n\pi$). It can be clearly seen that the maximum value of intensity is higher for panel *a* than that of panel *b*. This can be attributed to higher QCs present for “ $\omega = 1$ and $T = 0.005$ ” as compared to the QCs for “ $\omega = 1$ and $T = 1$ ” (see Fig. 3). This result is significant in light of the fact that for a specific combination of inter atomic spacing and observation angle, superradiant light can be observed for quantum mechanically correlated systems.

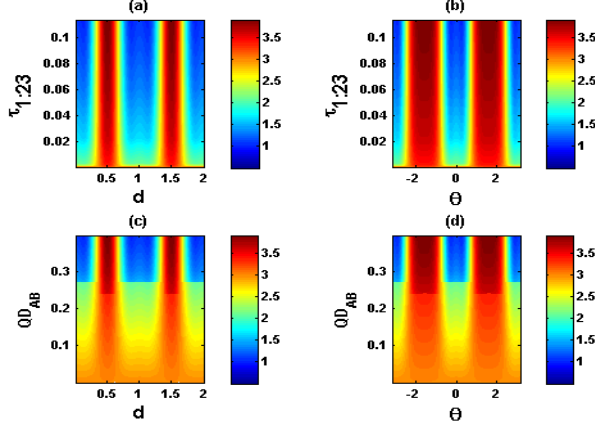


FIG. 5. (Color online) Panels *a* and *b* show intensity variation with respect to monogamy score of negativity, while panels *c* and *d* depict the radiation intensity with quantum discord for $T = 0.005$.

The contour plots of intensity as functions of QCs are depicted in Fig. 5 for temperature $T = 0.005$. Panels *a* and *b* show relation of intensity with monogamy score [51, 52] of negativity ($\tau_{1,23}$) [53], another measure of entanglement. It is observed that lower the temperature, higher is the monogamy score of negativity and stronger is the superradiance (for $d = \frac{\lambda}{2}$ and $\theta = \frac{\pi}{2}$). This clearly shows the relevance of monogamy relations in a physical scenario. Panels *c* and *d* show the variation of intensity with quantum discord, showing the sudden jump of intensity from sub- to super-radiant with increasing the amount of discord.

The analytical expression for the photon-photon correlation and the plots of these for different values of parameters, showing sub- and super-Poissonian statistics, are presented in supplementary material. It is evident that photon-statistics can be controlled parametrically.

IV. THE INTENSITY CHARACTERISTICS OF THE LOOP-CONFIGURATION

The far-field intensity pattern corresponding to the loop configuration shows entirely different behavior from that of the line-configuration. The schematic of the loop configuration is shown in Fig. 8(b), where the relative optical phase accumulated by a photon emitted at \vec{R}_j and detected at \vec{r} is given by,

$$\phi_1(\vec{r}) \equiv \phi_1 = k\vec{n} \cdot \vec{R}_1 = kd \sin \theta,$$

$$\phi_2(\vec{r}) \equiv \phi_2 = k\vec{n} \cdot \vec{R}_2 = 2kd \sin \theta,$$

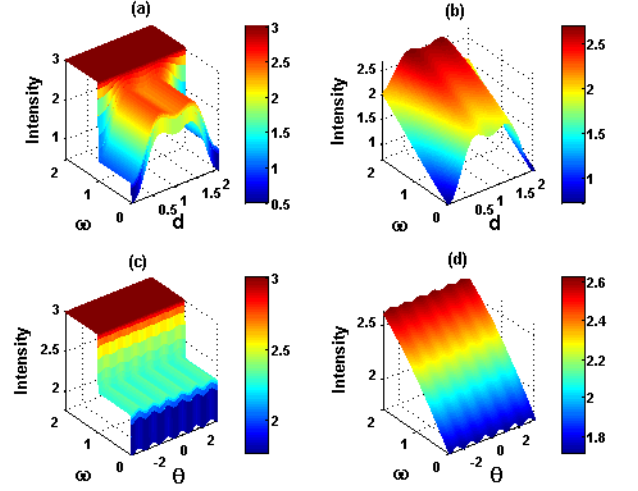


FIG. 6. (Color online) Panels *a* and *b* show the behavior of intensity for fixed observation angle ($\theta = \frac{\pi}{2}$) as a function of inter-atomic spacing and transition frequency for (a) $T=0.005$ and (b) $T=1$. Panels *c* and *d* show the intensity variation for fixed inter-atomic spacing ($d = \frac{\lambda}{2}$) as a function of observation angle and transition frequency for (c) $T=0.005$ and (d) $T=1$, showing the presence of uniform and non-uniform phases.

and

$$\phi_3(\vec{r}) \equiv \phi_3 = k\vec{n} \cdot \vec{R}_3 = \frac{3kd \sin \theta + \sqrt{3}kd \cos \theta}{2}. \quad (8)$$

Here the coupling, Ω_{ij} , is $\Omega_{12} = \Omega_{23} = \Omega_{13} = \Omega = 1$ and transition frequencies of all the atoms are taken to be same i. e., $\omega_1 = \omega_2 = \omega_3 = \omega$.

The intensity profile for the loop configuration is shown in Fig. 6 for two different temperatures. As is evident, the intensity is nearly independent of the observation angle. A jump in the intensity can be seen for lower temperature (see Fig. 6(c)), which is analogous to a quantum switch. This can have applications in control switching from high intensity to sub-radiant behavior. This feature disappears with increasing temperature due to thermal smearing as seen in Fig. 6(b). It is evident that emitted intensity for non-uniform phase is sub-radiant.

V. CONCLUSION

In conclusion, the emitted radiation from a coupled three particle system is shown to be a rich source of light of desired characteristics. It can be both uniform and highly focused in the far field regime in a controlled manner. The highly focused light owes its origin to QCs and can find application for lithography [3] and other technological applications. Apart from revealing the physical signature of quantum discord on the behavior of light, our investigation shows for the first time, the effect of three body correlation in the form of ‘monogamy

score’ on super-radiance. The shareability of QCs in a multipartite system is recorded through monogamy, which directly affects the radiation intensity. The fact that monogamy physically represents ‘sharing’ of quantum correlation in a multi-party channel and is found here to directly control the superradiant character of the intensity suggests the use of superradiance as a ‘QC sharing witness’ in a multi-party network. This may find application in the use of multiparty entanglement for secure information sharing and communication. The precise ‘witness’ character of monogamy score and the measurable property of superradiance reflecting the same are currently under investigation and will be reported elsewhere. We have obtained the exact expression for the radiation intensity and photon-photon correlation in the far field domain for three atoms at finite temperature. The photon-photon correlation demonstrates the sub- and super-Poissonian statistics of emitted radiation and the fact that it can be controlled by tuning the system parameters. The effect of quantum correlations

on emitted light, viz., concurrence, quantum discord, and monogamy score is explicitly demonstrated. The radiative behavior shows dramatic variation as a function of concurrence, quantum discord, and monogamy score of negativity, revealing the role of distinct QCs, thereby providing an optical probe for studying the quantum characteristics of emitting sources. Conditions under which hyper-radiance can be achieved is under investigation and also extension of this study to open quantum systems.

VI. ACKNOWLEDGEMENTS

Mithilesh K. Parit acknowledges discussion with Dr. Chiranjib Mitra and Department of Science and Technology, New Delhi, India for providing the DST-INSPIRE fellowship during his stay at IISER Kolkata.

-
- [1] G. Grynberg, A. Aspect, and C. Fabre, *Introduction to Quantum Optics: From the Semi-classical Approach to Quantized Light*, (Cambridge University Press, Cambridge, UK), 2010.
 - [2] G. S. Agarwal, *Quantum Optics* (Cambridge University Press, Cambridge, UK), 2013.
 - [3] A. N. Boto, P. Kok, D. S. Abrams, S. L. Braunstein, C. P. Williams, and J. P. Dowling, Phys. Rev. Lett. **85**, 2733 (2000).
 - [4] M. Schiavon, G. Vallone, F. Ticozzi, and P. Villoresi, Phys. Rev. A **93**, 012331 (2016).
 - [5] X. Zhang, C. Xu, and Z. Ren, Nature, Scientific Reports, **8**, 3140 (2018) and references therein.
 - [6] J. W. Pan, D. Bouwmeester, H. Weinfurter, and A. Zeilinger, Phys. Rev. Lett. **80**, 3891 (1998).
 - [7] T. Jennewein, C. Simon, G. Weihs, H. Weinfurter, and A. Zeilinger, Phys. Rev. Lett. **84**, 4729 (2000).
 - [8] W. Tittel, J. Brendel, H. Zbinden, and N. Gisin, Phys. Rev. Lett. **84**, 4737 (2000).
 - [9] A. Lamas-Linares, J. C. Howell, and D. Bouwmeester, Nature **412**, 887890 (2001).
 - [10] A. Poppe, A. Fedrizzi, R. Ursin, H. R. Bhm, T. Lornser, O. Maurhardt, M. Peev, M. Suda, C. Kurtsiefer, H. Weinfurter, T. Jennewein, and A. Zeilinger, Opt. Express **12**, 3865-3871 (2004).
 - [11] M. Sttzt, S. Grblacher, T. Jennewein, and A. Zeilinger, Appl. Phys. Lett. **90**, 261114 (2007).
 - [12] A. R. Usha Devi and A. K. Rajagopal, Phys. Rev. A **79**, 062320 (2009).
 - [13] A. Zeilinger, Phys. Scr. **92**, 072501 (2017) and references therein.
 - [14] J. P. W. MacLean, J. M. Donohue, and K. J. Resch, Phys. Rev. A **97**, 063826 (2018).
 - [15] J. P. W. MacLean, J. M. Donohue, and K. J. Resch, Phys. Rev. Lett. **120**, 053601 (2018).
 - [16] R. H. Dicke, Phys. Rev. **93**, 99 (1954).
 - [17] R. Wiegner, J. von-Zanthier, and G. S. Agarwal, Phys. Rev. A **84**, 023805 (2011).
 - [18] N. Skribanowitz, I. P. Herman, J. C. MacGillivray, and M. S. Feld, Phys. Rev. Lett. **30**, 309 (1973).
 - [19] M. O. Scully, E. S. Fry, C. H. R. Ooi, and K. Wodkiewicz, Phys. Rev. Lett. **96**, 010501 (2006).
 - [20] E. A. Sete, A. A. Svidzinsky, H. Eleuch, Z. Yang, R. D. Neels, and M. O. Scully, J. Mod. Opt. **57** (14-15), 1311 (2010).
 - [21] R. Bonifacio, N. Piovela, and B. W. J. McNeil, Phys. Rev. A **44**, R3441(R)(1991).
 - [22] E. Prat, L. Florian, and S. Reiche, Phys. Rev. ST Accel. Beams **18**, 100701 (2015).
 - [23] P. Sprangle and T. Coffey, Phys. Today **37**, No. 3, 44 (1984).
 - [24] M. Scheibner, T. Schmidt, L. Worschech, A. Forchel, G. Bacher, T. Passow, and D. Hommel, Nat. Phys. **3**, 106 (2007).
 - [25] M. Gross, C. Fabre, P. Pillet, and S. Haroche, Phys. Rev. Lett. **36**, 1035 (1976).
 - [26] A. Goban, C. L. Hung, J. D. Hood, S. P. Yu, J. A. Muniz, O. Painter, and H. J. Kimble, Phys. Rev. Lett. **115**, 063601 (2015).
 - [27] I. Dimitrova, W. Lunden, J. Amato-Grill, N. Jepsen, Y. Yu, M. Messer, T. Rigaldo, G. Puentes, D. Weld, and W. Ketterle, Phys. Rev. A, **96**, 051603(R) (2017).
 - [28] D. Bhatti, R. Schneider, S. Oppel, and J. von Zanthier, Phys. Rev. Lett., **120**, 113603 (2018).
 - [29] F. Mivehvar, S. Ostermann, F. Piazza, and H. Ritsch, Phys. Rev. Lett. **120**, 123601 (2018).
 - [30] A. Biswas and G. S. Agarwal, J. Mod. Opt. **51**, 1627 (2004).
 - [31] D. D. B. Rao, P. K. Panigrahi, and C. Mitra, Phys. Rev. A **78**, 022336 (2008).
 - [32] D. Porras and J. I. Cirac, Phys. Rev. A **78**, 053816 (2008).
 - [33] B. Casabone, K. Friebe, B. Brandstatter, K. Schuppert, R. Blatt, and T. E. Northup, Phys. Rev. Lett. **114**, 023602 (2015).
 - [34] R. Reimann, W. Alt, T. Kampschulte, T. Macha, L.

- Ratschbacher, N. Thau, S. Yoon, and D. Meschede, Phys. Rev. Lett. **114**, 023601 (2015).
- [35] M. D. Eisaman, A. Andre, F. Massou, M. Fleischhauer, A. S. Zibrov, and M. D. Lukin, Nature (London) **438**, 837 (2005).
- [36] A. Kalachev and S. Kroll, Phys. Rev. A **74**, 023814 (2006).
- [37] A. Kalachev, Phys. Rev. A **76**, 043812 (2007).
- [38] V. Vedral, Nature Physics **10**, 256-258 (2014) and references therein.
- [39] C. Mitra, Nature Physics **11**, 212-213 (2015).
- [40] D. Das, H. Singh, T. Chakraborty, R. K. Gopal, and C. Mitra, New J. Phys. **15** 013047 (2013).
- [41] H. Singh, T. Chakraborty, P. K. Panigrahi, and C. Mitra, Quantum Inf Process **14**, 951961 (2015).
- [42] D. M. Greenberger, M. A. Horne, and A. Zeilinger, *Bell's Theorem, Quantum Theory, and Conceptions of the Universe*, Kluwer Academics, The Netherlands, 73-76 (1989).
- [43] V. S. Bhaskara and P. K. Panigrahi, Quantum Inf Process **16**, 118 (2017) and references therein.
- [44] S. Q. Tang, J. B. Yuan, L. M. Kuang, and X. W. Wang, Quantum Inf Process **14**, 2883 (2015).
- [45] S. Banerjee, V. Ravishankar, and R. Srikanth, Ann. Phys. **325**, 816 (2010).
- [46] S. Banerjee, V. Ravishankar, and R. Srikanth, Eur. Phys. J. D **56**, 277290 (2010).
- [47] W. K. Wootters, Phys. Rev. Lett. **80**, 2245 (1998).
- [48] H. Ollivier and W. H. Zurek, Phys. Rev. Lett. **88**, 017901 (2001).
- [49] L. Henderson and V. Vedral, J. Phys. A: Math. Gen. **34**, 6899 (2001).
- [50] S. Luo, Phys. Rev. A **77**, 042303 (2008).
- [51] V. Coffman, J. Kundu, and W. K. Wootters Phys. Rev. A **61**, 052306 (2000).
- [52] M. N. Bera, R. Prabhu, A. Sen(De), and U. Sen, Phys. Rev. A **86**, 012319 (2012).
- [53] G. Vidal and R. F. Werner, Phys. Rev. A **65**, 032314 (2002).

SUPPLEMENTARY INFORMATION: QUANTUM LIGHT ON DEMAND

VII. THE MODEL

We consider a system of three coupled identical atoms, where the excited state $|e_i\rangle$ and the ground state $|g_i\rangle$, $i = 1, 2, 3$ are separated by an energy interval $\hbar\omega$. The Hamiltonian for the system of three identical two-level atoms coupled through dipole-dipole interaction is given by,

$$H = \sum_{i=1}^3 \omega_i S_i^z + \sum_{i \neq j=1}^3 \Omega_{ij} S_i^+ S_j^- . \quad (9)$$

The schematic representation of the two configurations are shown below:

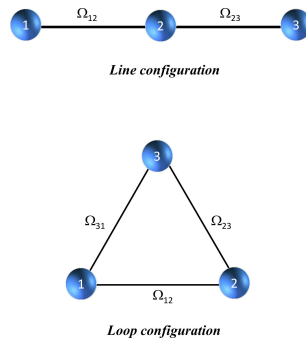


FIG. 7. (Color online) Schematic representation of topologically distinct line (open loop) and loop (closed loop) configurations for three qubits coupled via dipole-dipole interaction.

where the partition function Z is given by

$$Z = e^{\frac{3\omega}{2k_B T}} + e^{\frac{-3\omega}{2k_B T}} + e^{\frac{(\frac{\omega}{2} - \sqrt{2}\Omega)}{k_B T}} + e^{\frac{-(\frac{\omega}{2} + \sqrt{2}\Omega)}{k_B T}} + e^{\frac{(\frac{\omega}{2} + \sqrt{2}\Omega)}{k_B T}} + e^{\frac{-(\frac{\omega}{2} - \sqrt{2}\Omega)}{k_B T}} + e^{\frac{\omega}{2k_B T}} + e^{\frac{-\omega}{2k_B T}}.$$

The non-vanishing density matrix elements of $\rho_{ABC}(T)$ are given by

$$\begin{aligned} \rho_{11} &= e^{\frac{3\omega}{2k_B T}}; \quad \rho_{88} = e^{\frac{-3\omega}{2k_B T}} \\ \rho_{22} = \rho_{44} &= \frac{1}{4} \left[e^{\frac{(\frac{\omega}{2} - \sqrt{2}\Omega)}{k_B T}} + e^{\frac{(\frac{\omega}{2} + \sqrt{2}\Omega)}{k_B T}} + 2e^{\frac{\omega}{2k_B T}} \right]; \quad \rho_{33} = \frac{1}{2} \left[e^{\frac{(\frac{\omega}{2} - \sqrt{2}\Omega)}{k_B T}} + e^{\frac{(\frac{\omega}{2} + \sqrt{2}\Omega)}{k_B T}} \right] \\ \rho_{55} = \rho_{77} &= \frac{1}{4} \left[e^{-(\frac{\omega}{2} - \sqrt{2}\Omega)k_B T} + e^{-\frac{(\frac{\omega}{2} + \sqrt{2}\Omega)}{k_B T}} + 2e^{-\frac{\omega}{2k_B T}} \right]; \quad \rho_{66} = \frac{1}{2} \left[e^{-\frac{(\frac{\omega}{2} - \sqrt{2}\Omega)}{k_B T}} + e^{-\frac{(\frac{\omega}{2} + \sqrt{2}\Omega)}{k_B T}} \right] \\ \rho_{23} = \rho_{34} &= \frac{1}{2\sqrt{2}} \left[e^{\frac{(\frac{\omega}{2} - \sqrt{2}\Omega)}{k_B T}} - e^{\frac{(\frac{\omega}{2} + \sqrt{2}\Omega)}{k_B T}} \right]; \quad \rho_{24} = \frac{1}{4} \left[e^{\frac{(\frac{\omega}{2} - \sqrt{2}\Omega)}{k_B T}} + e^{\frac{(\frac{\omega}{2} + \sqrt{2}\Omega)}{k_B T}} - 2e^{\frac{\omega}{2k_B T}} \right] \\ \rho_{56} = \rho_{67} &= \frac{1}{2\sqrt{2}} \left[e^{-\frac{(\frac{\omega}{2} + \sqrt{2}\Omega)}{k_B T}} - e^{-\frac{(\frac{\omega}{2} - \sqrt{2}\Omega)}{k_B T}} \right]; \quad \rho_{57} = \frac{1}{4} \left[e^{-\frac{(\frac{\omega}{2} + \sqrt{2}\Omega)}{k_B T}} + e^{-\frac{(\frac{\omega}{2} - \sqrt{2}\Omega)}{k_B T}} - 2e^{-\frac{\omega}{2k_B T}} \right]. \end{aligned} \quad (13)$$

From the above description, one observes that the system at high temperature is perfectly separable. However, for intermediate temperatures, the system is in a mixed state and we have investigated the intensity pattern and photon-photon correlation of such a system. We have used $k_B = 1$ in our calculation.

In the line configuration intensity, I , is given by

$$I = \langle E^- E^+ \rangle = A (B + C + D),$$

with

$$\begin{aligned} A &= \frac{e^{-\frac{\omega}{2T}} \text{sech}\left(\frac{\omega}{2T}\right)}{2 \left(1 + 2 \cosh\left(\frac{\omega}{T}\right) + 8 \cosh\left(\frac{\sqrt{2}\Omega}{T}\right)\right)}, \quad B = 3e^{\frac{2\omega}{T}} - 2e^{\frac{\omega}{T}} (-2 + \cos(2k\text{dsin}(\theta))), \\ C &= 4 \left(2 + \cos(2k\text{dsin}(\theta)) + e^{\frac{\omega}{T}} (4 + \cos(2k\text{dsin}(\theta)))\right) \cosh\left(\frac{\sqrt{2}\Omega}{T}\right), \quad \text{and} \\ D &= 4 \sin^2(k\text{dsin}(\theta)) - 8\sqrt{2} \left(1 + e^{\frac{\omega}{T}}\right) \cos(k\text{dsin}(\theta)) \sinh\left(\frac{\sqrt{2}\Omega}{T}\right). \end{aligned} \quad (14)$$

The exact expression of photon-photon or intensity-intensity correlation is given by

$$g^{(2)}(0) = \frac{\langle E^- E^- E^+ E^+ \rangle}{\langle E^- E^+ \rangle \langle E^- E^+ \rangle}. \quad (15)$$

The numerator in Eq. (15) is given by

$$\langle E^- E^- E^+ E^+ \rangle = N_1 (N_2 + N_3),$$

with

$$\begin{aligned} N_1 &= \frac{e^{2k\text{dsin}(\theta) + \frac{\omega - \sqrt{2}\Omega}{2T}} \text{sech}\left(\frac{\omega}{2T}\right)}{2 \left(1 + 2 \cosh\left(\frac{\omega}{T}\right) + 8 \cosh\left(\frac{\sqrt{2}\Omega}{T}\right)\right)}, \\ N_2 &= -4\sqrt{2} \left(-1 + e^{\frac{2\sqrt{2}\Omega}{T}}\right) \cos(k\text{dsin}(\theta)) + 2 (2 + \cos(2k\text{dsin}(\theta))), \quad \text{and} \\ N_3 &= e^{\frac{2\sqrt{2}\Omega}{T}} \left(4 + 3e^{\frac{2\omega}{T}} + 2\cos(2k\text{dsin}(\theta))\right) + 4e^{\frac{\sqrt{2}\Omega}{T}} \sin^2(k\text{dsin}(\theta)). \end{aligned} \quad (16)$$

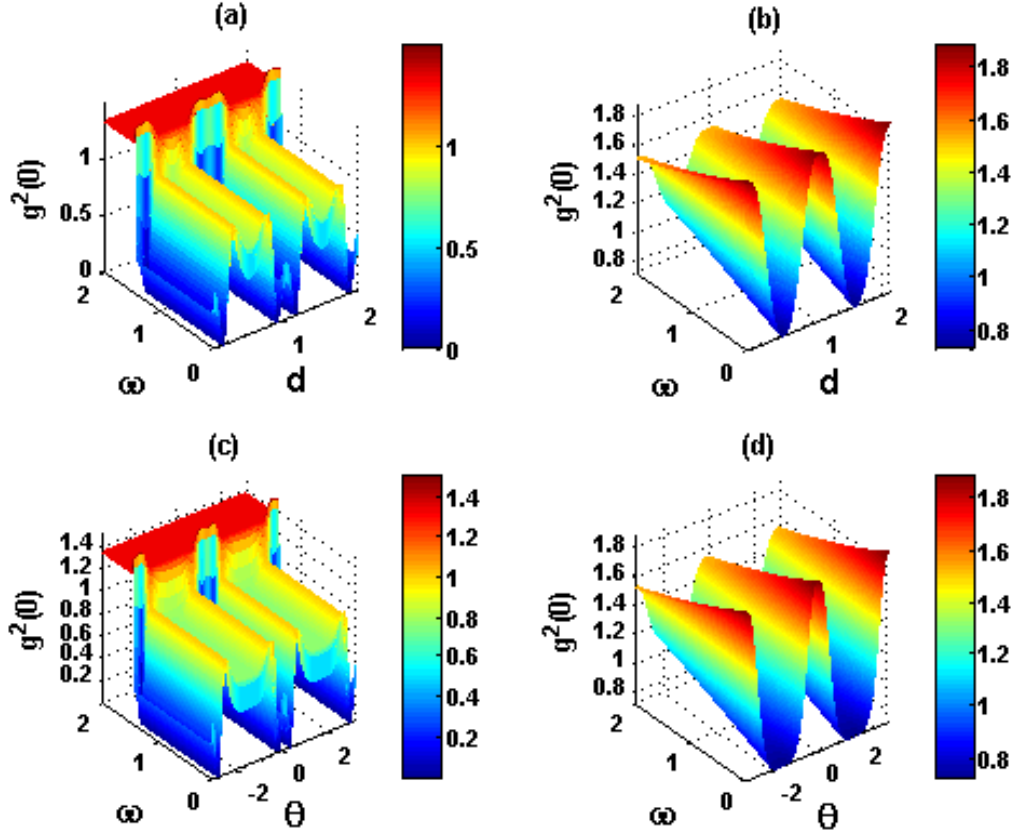


FIG. 9. (Color online) Panels *a* and *b* show the variation of photon-photon correlation at fixed temperature and inter-atomic spacing ($d = \frac{\lambda}{2}$) as a function of observation angle and transition frequency for (a) $T=0.005$ and (b) $T=1$. Panels *c* and *d* show the intensity variation at fixed temperature and observation angle as a function of inter-atomic spacing and transition frequency for (c) $T=0.005$ and (d) $T=1$.

The Figures (9) and (10) show the photon statistics ($g^2(0)$) of the three atoms placed along the line. The value of $g^2(0) < 1$ shows sub Poissonian behavior and $g^2(0) > 1$ shows super Poissonian behavior.

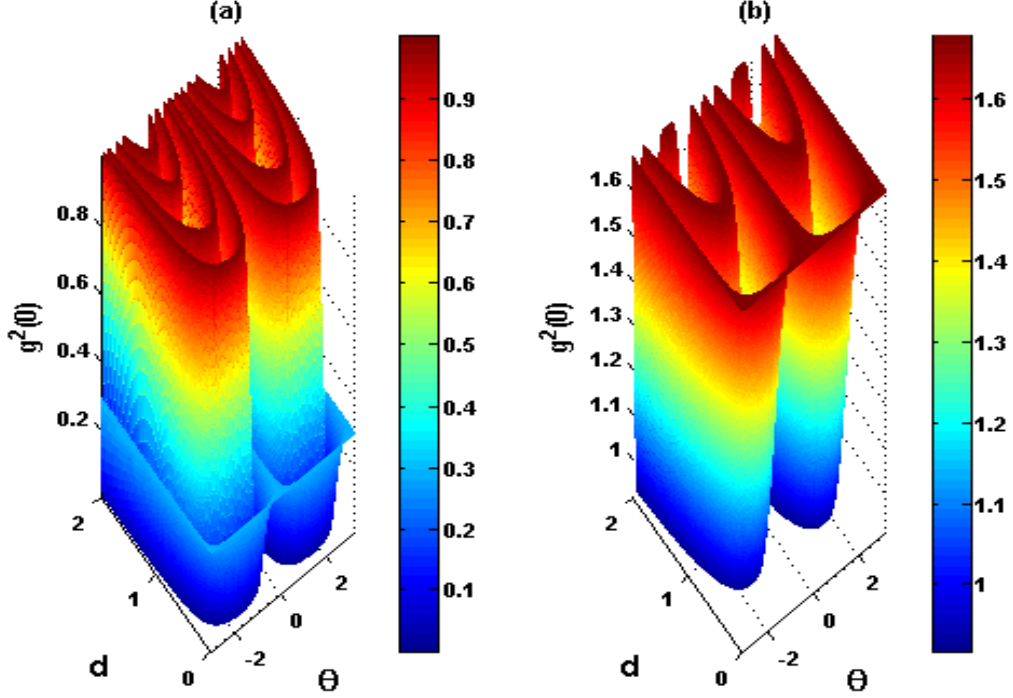


FIG. 10. (Color online) The variation of photon-photon correlation as a function of observation angle and spacing between atoms at fixed transition frequency ($\omega = 1$) for different temperatures of magnitude (a) $T = 0.005$ and (b) $T = 1$ is shown here.

IX. PHOTON-PHOTON CORRELATION IN LOOP CONFIGURATION

In this section, we present the eigenvalues, eigenstates, and non-vanishing terms of thermal density matrix of dipole coupled two-level atoms, placed at the vertices of the equilateral triangle. The eigenvalues of the Hamiltonian with $\Omega_{12} = \Omega_{23} = \Omega_{13} = \Omega$ are given by,

$$\epsilon_1 = \frac{-3\omega}{2}; \quad \epsilon_2 = -\Omega - \frac{\omega}{2}; \quad \epsilon_3 = -\Omega - \frac{\omega}{2}; \quad \epsilon_4 = 2\Omega - \frac{\omega}{2}$$

$$\epsilon_5 = \frac{\omega}{2} - \Omega; \quad \epsilon_6 = \frac{\omega}{2} - \Omega; \quad \epsilon_7 = \frac{\omega}{2} + 2\Omega; \quad \epsilon_8 = \frac{3\omega}{2}$$

and the corresponding eigenstates $|\phi_i\rangle$ of the system are given by

$$\begin{aligned} |\phi_1\rangle &= |g_1 g_2 g_3\rangle; \quad |\phi_2\rangle = \frac{1}{\sqrt{2}} [|g_1 e_2 g_3\rangle - |e_1 g_2 g_3\rangle] \\ |\phi_3\rangle &= \frac{1}{\sqrt{2}} [|g_1 g_2 e_3\rangle - |e_1 g_2 g_3\rangle]; \quad |\phi_4\rangle = \frac{1}{\sqrt{3}} [|e_1 g_2 g_3\rangle + |g_1 e_2 g_3\rangle + |g_1 g_2 e_3\rangle] \\ |\phi_5\rangle &= \frac{1}{\sqrt{2}} [|e_1 g_2 e_3\rangle - |e_1 e_2 g_3\rangle]; \quad |\phi_6\rangle = \frac{1}{\sqrt{2}} [|g_1 e_2 e_3\rangle - |e_1 e_2 g_3\rangle] \\ |\phi_7\rangle &= \frac{1}{\sqrt{3}} [|e_1 e_2 g_3\rangle + |e_1 g_2 e_3\rangle + |g_1 e_2 e_3\rangle]; \quad |\phi_8\rangle = |e_1 e_2 e_3\rangle. \end{aligned}$$

One can obtain the temperature dependent density matrix elements and the non-vanishing density matrix elements

thus obtained are listed below,

$$\begin{aligned}
 \rho_{11} &= e^{\frac{3\omega}{2k_B T}}; \quad \rho_{88} = e^{\frac{-3\omega}{2k_B T}} \\
 \rho_{22} &= \frac{1}{3}e^{\frac{(\frac{\omega}{2}-2\Omega)}{k_B T}} + e^{\frac{(\frac{\omega}{2}+\Omega)}{k_B T}}; \quad \rho_{33} = \rho_{44} = \frac{1}{3}e^{\frac{(\frac{\omega}{2}-2\Omega)}{k_B T}} + \frac{1}{2}e^{\frac{(\frac{\omega}{2}+\Omega)}{k_B T}} \\
 \rho_{55} &= \frac{1}{3}e^{-\frac{(\frac{\omega}{2}+2\Omega)}{k_B T}} + e^{-\frac{(\frac{\omega}{2}-\Omega)}{k_B T}}; \quad \rho_{66} = \rho_{77} = \frac{1}{3}e^{-\frac{(\frac{\omega}{2}+2\Omega)}{k_B T}} + \frac{1}{2}e^{-\frac{(\frac{\omega}{2}-\Omega)}{k_B T}} \\
 \rho_{23} &= \rho_{24} = \frac{1}{3}e^{\frac{(\frac{\omega}{2}-2\Omega)}{k_B T}} - \frac{1}{2}e^{\frac{(\frac{\omega}{2}+\Omega)}{k_B T}}; \quad \rho_{34} = \frac{1}{3}e^{\frac{(\frac{\omega}{2}-2\Omega)}{k_B T}} \\
 \rho_{56} &= \rho_{57} = \frac{1}{3}e^{-\frac{(\frac{\omega}{2}+2\Omega)}{k_B T}} - \frac{1}{2}e^{-\frac{(\frac{\omega}{2}-\Omega)}{k_B T}}; \quad \rho_{67} = \frac{1}{3}e^{-\frac{(\frac{\omega}{2}+2\Omega)}{k_B T}}.
 \end{aligned} \tag{17}$$

The partition function for this system is given by,

$$Z = e^{\frac{3\omega}{2k_B T}} + e^{\frac{-3\omega}{2k_B T}} + e^{\frac{(\frac{\omega}{2}-2\Omega)}{k_B T}} + e^{-\frac{(\frac{\omega}{2}+2\Omega)}{k_B T}} + 2e^{\frac{(\frac{\omega}{2}+\Omega)}{k_B T}} + 2e^{-\frac{(\frac{\omega}{2}-\Omega)}{k_B T}}.$$

At high temperature, the density matrix reduces to a mixed state, which can not be written in terms of product states.

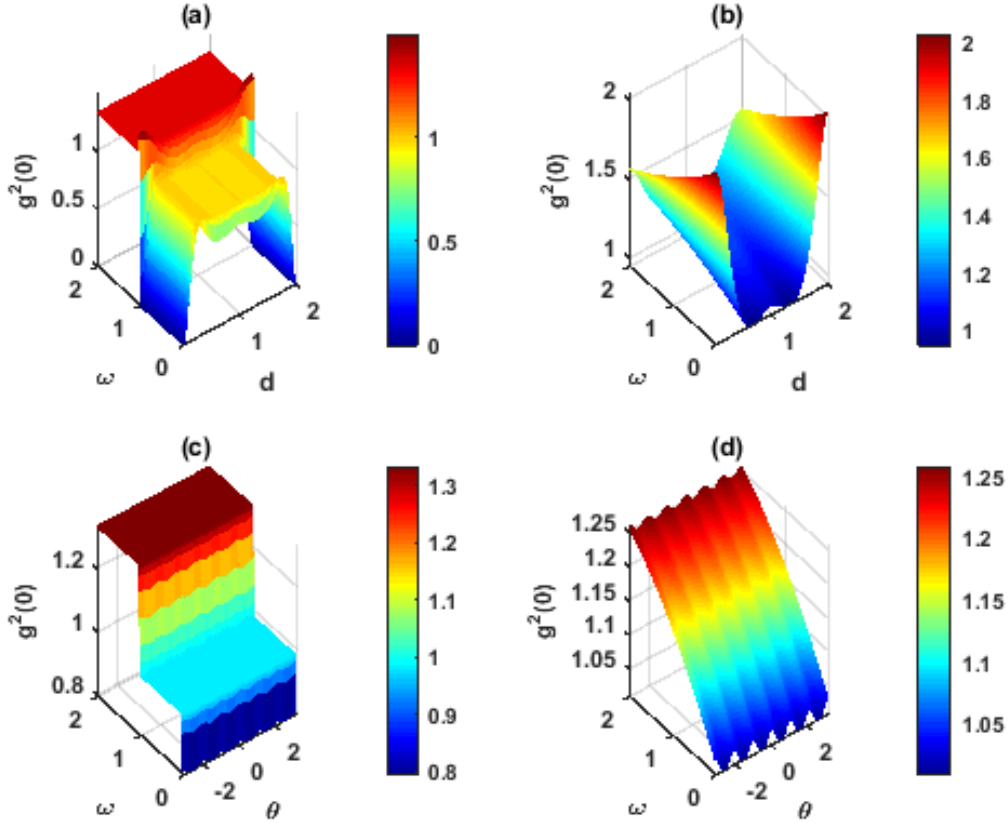


FIG. 11. (Color online) Panels *a* and *b* show the variation of photon-photon correlation at fixed temperature and inter-atomic spacing ($d = \frac{\lambda}{2}$) as a function of observation angle and transition frequency for (a) $T=0.005$ and (b) $T=1$. Panels *c* and *d* show the intensity variation at fixed temperature and observation angle as a function of inter-atomic spacing and transition frequency for (c) $T=0.005$ and (d) $T=1$.

The Figures (11) and (12) show the photon statistics ($g^2(0)$) of the three atoms placed along the line. The value of $g^2(0) < 1$ shows sub Poissonian behavior and $g^2(0) > 1$ shows super Poissonian behavior.

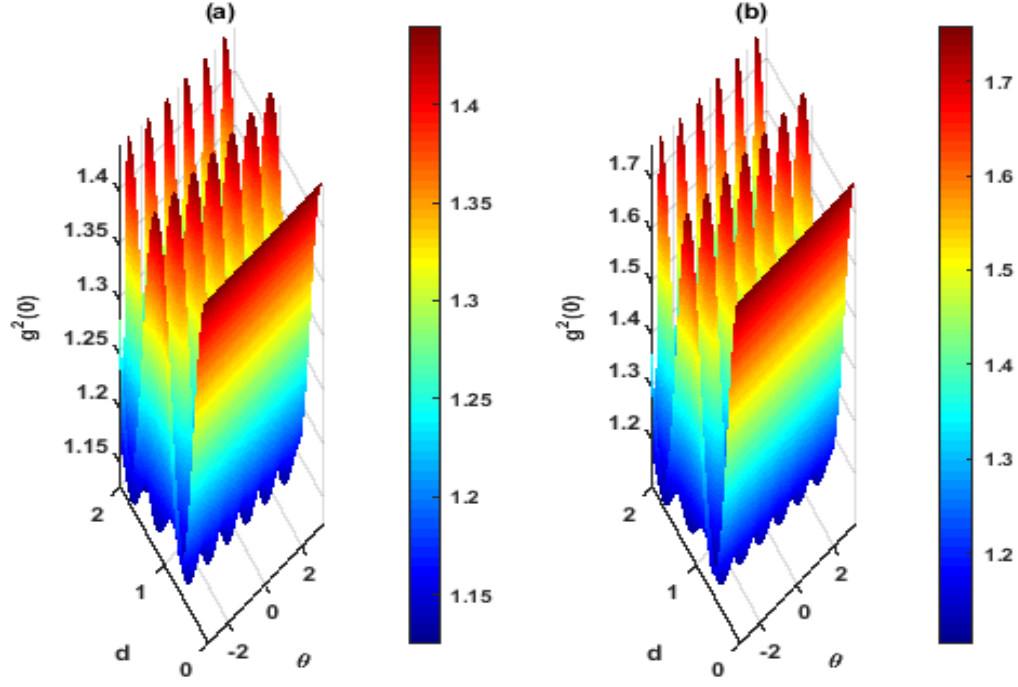


FIG. 12. (Color online) The variation of photon-photon correlation as a function of observation angle and spacing between atoms at fixed transition frequency ($\omega = 1$) for different temperatures of magnitude (a) $T = 0.005$ and (b) $T = 1$ is shown here.